HYPERSPECTRAL IMAGING TECHNOLOGY FOR WOUND CARE

ABSTRACT

"Noninvasive imaging approaches can provide greater information about a wound than visual inspection during the wound healing and treatment process. These assessments are achieved through quantitative optical analysis of tissue characteristics including blood flow, collagen remodeling, hemoglobin content, inflammation, temperature, vascular structure, and water content. The noninvasive optical imaging approach includes hyperspectral imaging, multispectral imaging, near-infrared spectroscopy (NIRS), diffuse reflectance spectroscopy, optical coherence tomography, laser Doppler imaging, laser speckle imaging, spatial frequency domain imaging, and fluorescence imaging. The various wounds imaged using these techniques include open wounds, chronic wounds, diabetic foot ulcers, decubitus ulcers, venous leg ulcers, and burns. All the technologies are currently at various stages of translational efforts to the clinic, with NIRS holding a greater promise for physiological assessment of the wounds internal, beyond the gold-standard visual assessment. NIRS has the potential to penetrate deeper, demonstrating the potential to image internal wounds"

Anthony C. Dike, FACP, FASPC

HYPER SPECTRAL IMAGER SPECIFICATION DOCUMENT

The diagram below schematically depicts the various components of a typical hyperspectral imaging system. The illumination optics should consist of:

(1) Nine broadband visible light-emitting diodes (LEDs) (XR-E WHT-L1, Cree, Inc., Durham, NC) emitting primarily between 500 and 700 nm, and

(2) collimating wide lenses (OP-025, Dialight Corp., North Yorkshire, United Kingdom).

The LEDs should be arranged radially around the collection optics and should be cross-polarized relative to the collection optics. The diffuse reflectance will be measured by eliminating the Fresnel reflection in the images. This could be achieved by placing a linear polarizer film (XP38, Optical Filters Ltd., Meadville, PA), set between two acrylic sheets in front of the LED assembly.

The collection optics will be composed of :

(1) a spectral separator (LCTF-10-20, CRI Inc., Woburn, MA),

(2) a charge-coupled device (CCD) (Guppy F-1468, Allied Vision Technologies, Stadtroda, Germany), and

(3) a 25 mm focal length imaging lens (MFA2514, SENKO Advanced Components, Inc., Marlboro, MA).

The spectral separator will be tunable over the range of 400–720 nm with a full width at half maximum of 10 nm and also will act as a linear polarizer. The detection system will be designed with an 18-inch focal length and a spatial resolution of at least 100 μm.

<u>Schematic of the different components of the proposed hyperspectral imager</u>
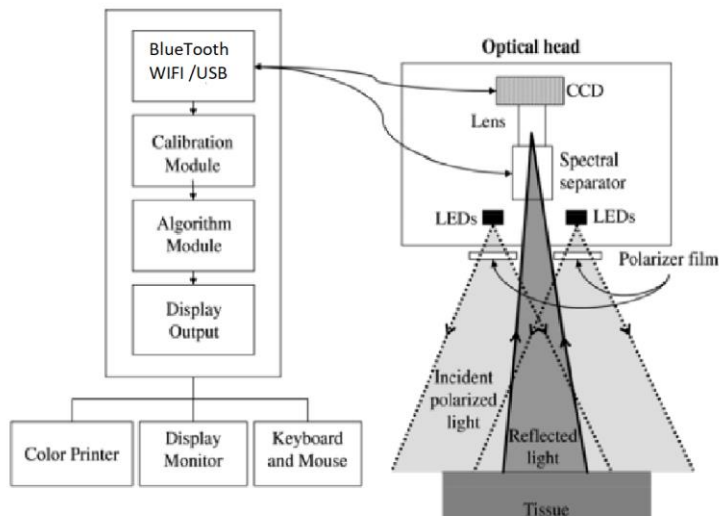
EXPERIMENTAL SETUP AND PROCEDURE

Subjects will be imaged supine on a standard examination table or reclining chair. A fiducial target will be placed near the center of the imager's field of view to correct for movement of the foot during the hypercube acquisition. For each measurement site, the hyperspectral imager will collect two hypercubes corresponding to either background $Btissue(x,y, \lambda j)$ or LED-illuminated conditions $Itissue(x,y, \lambda j)$. The spectral separator will be tuned to 15 equally spaced wavelengths between 500 and 660 nm while the CCD measured the tissue reflectance. The LEDs will be switched off and on to produce both illumination conditions, respectively. Acquisition at each wavelength should last for approximately 1 second. To normalize and correct for spectral variation in illumination intensity and collector sensitivity, the hyperspectral imager will be calibrated to a well-characterized, highly and diffusely reflecting standard prior to imaging every subject. The same procedure will be used to acquire background and illuminated calibration hypercubes denoted by $Bcalib(x,y, \lambda j)$ and $Icalib(x,y, \lambda j)$, respectively. Then, the diffuse reflectance used to determined the absorptance $Aobs(x,y,lj)$ of the tissues given by **Equation (1)**, will be computed as

$$R_d(x, y, \lambda_j) = \frac{I_{tissue}(x, y, \lambda_j) - B_{tissue}(x, y, \lambda_j)}{I_{calib}(x, y, \lambda_j) - B_{calib}(x, y, \lambda_j)}$$

The OXY and DEOXY values will be reported by the device in arbitrary units and estimated using Method 1 (as described in detail below)from reflectance measurements at 15 wavelengths were validated against those obtained from high resolution spectrometric measurements and retrieving *Moxy* and *Mdeoxy* in units of mmol/liter in a manner similar to that described by Gillies *et al*. Oximetry data will be gathered simultaneously with both devices from eight anatomical sites pre- and post-pressure cuff-induced ischemia on the dorsal feet of test healthy subjects. The values of OXY and DEOXY should be linearly proportional to *Moxy* and *Mdeoxy* with correlation coefficients of about 0.86 and 0.88, respectively. This should confirm that the OXY and DEOXY values reported by the device are strong indicators of the actual molar concentrations of oxyhemoglobin and deoxyhemoglobin, albeit in arbitrary units.

Method 1. Modified Beer-Lambert Law and Calibration

The modified Beer–Lambert law (MBLL) is the basis of continuous-wave near-infrared tissue spectroscopy (cwNIRS). The differential form of MBLL (dMBLL) states that the change in light attenuation is proportional to the changes in the concentrations of tissue chromophores, mainly oxy- and deoxyhaemoglobin. If attenuation changes are measured at two or more wavelengths, concentration changes can be calculated. The dMBLL is based on two assumptions: (1) the absorption of the tissue changes homogeneously, and (2) the scattering loss is constant. It is known that absorption changes are usually inhomogeneous, and therefore dMBLL underestimates the changes in concentrations (partial volume effect) and every calculated value is influenced by the change in the concentration of other chromophores (cross-talk between chromophores). However, the error introduced by the second assumption (cross-talk of scattering changes) has not been assessed previously. An analytically treatable special case (semi-infinite, homogeneous medium, with optical properties of the cerebral cortex) was utilized to estimate its order of magnitude. This showed that the per cent change of the transport scattering

coefficient and that of the absorption coefficient have an approximately equal effect on the changes of attenuation, and a 1% increase in scattering increases the estimated concentration changes by about 0.5 µM.

The so-called apparent absorption of the tissue $A_{obs}(x,y, \lambda_j)$ at the spatial coordinate (x,y) and at wavelength λ_j can be calculated using the modified Beer-Lambert law as

$$A_{obs}(x, y, \lambda_j) = -\log_{10}[R_d(x, y, \lambda_j)]$$
(1)

where $R_d(x,y,\lambda_j)$ is the diffuse reflectance emerging around the normal direction and measured experimentally. The primary chromophores in the human skin responsible for absorption of visible light are oxyhemoglobin, deoxyhemoglobin, and melanin. Thus, the apparent absorption (or extinction) can be modeled as the sum of absorption from chromophores and scattering by the tissue:

$$A_{mod}(x, y, \lambda_j) = \varepsilon_{oxy}(\lambda_j)M_{oxy}(x, y)L + \varepsilon_{deoxy}(\lambda_j)M_{deoxy}(x, y)L + \varepsilon_{mel}(\lambda_j)M_{mel}(x, y)L + G$$
(2)

where $M_i(x,y)$ is the molar concentration of chromo- phore "i" at coordinate (x,y) (expressed in mol/liter) and $\varepsilon_i(\lambda)$ is a spectral molar absorption coefficient [in cm^{-1}/(mol/liter)] while the subscripts *oxy, deoxy*, and *mel* refer to oxyhemoglobin, deoxyhemoglobin, and melanin, respectively. The mean free path L (in centimeters) is the average distance traveled by a photon within the tissue before it reemerges out of the tissue. The term G accounts for light scattering by the skin outside of the acceptance angle of the collector optics; it depends on the geometry of the collector optics and can be assumed to be independent of wavelength. The spectral molar absorption coefficients $\varepsilon_{oxy}(\lambda_j)$, $\varepsilon_{deoxy}(\lambda_j)$, and $\varepsilon_{mel}(\lambda_j)$ were taken from the literature and are shown below. The mean free path L is unknown and so the products $M_{oxy}(x,y)L$, $M_{deoxy}(x,y)L$, and $M_{mel}(x,y)L$ can be substituted by effective concentrations OXY(x,y), DEOXY(x, y), and MEL(x, y), respectively. Then, the four unknown parameters OXY, DEOXY, MEL, and G can be retrieved at each location (x,y) by minimizing the residual r given by

$$r = \sum_{j=1}^{13}\{A_{obs}(\lambda_j) - s[OXY\varepsilon_{oxy}(\lambda_j) + DEOXY\varepsilon_{deoxy}(\lambda_j) + MEL\varepsilon_{mel}(\lambda_j)] + G\}^2$$
(3)

where the factor s was introduced to scale empirically the effective oxyhemoglobin concentration OXY to be 50 on average for a population of healthy subjects. Minimization of the residual r can be performed numerically with an optimization software such as the popular Levenberg-Marquardt algorithm. The effective total hemoglobin concentration, HEME, and the oxygen saturation, SO$_2$, at coordinate (x,y) are then calculated as HEME = OXY + DEOXY and SO2 = OXY/HEME, respectively.